RSC Advances

ROYAL SOCIETY OF CHEMISTRY

www.rsc.org/advances

Cite this: DOI: 10.1039/c0xx00000x

www.rsc.org/xxxxxx

ARTICLE TYPE

One–pot fabrication and thermoelectric properties of Ag nanoparticles /polyaniline hybrid nanocomposites

Weijie Wang , Suping Sun , Shijia Gu, Hongwei Shen, Qihao Zhang, Juanjuan Zhu, Lianjun Wang*, Wan Jiang

Received (in XXX, XXX) Xth XXXXXXXXX 20XX, Accepted Xth XXXXXXXXX 20XX
DOI: 10.1039/b000000x

It is well introduced in this context a one-pot and in-situ strategy for fabrication of AgNPs (Ag nanoparticles)/PANI (Polyaniline) nanocomposites in a micellar solution of dodecy benzene sulfonic acid (DBSA, anionic surfactant).Guided by this strategy, AgNPs was directly synthesized from silver nitrate. AgNPs/PANI hybrid nanocomposites with AgNPs were consolidated via spark plasma sintering (SPS). The phase structure and microstructure of the as-prepared composites were evaluated by several characterizations and then we speculated the growth mechanism of AgNPs. The thermoelectric properties of the samples containing increasing silver nitrate content were systematically investigated. Compared with pure bulk PANI, the thermoelectric performance of AgNPs/PANI hybrid nanocomposites exhibits a distinct enhancement for AgNPs adding. The Seebeck coefficient (S) decreased slightly while the electric conductivity (σ) was found to increase remarkably, and thermal conductivity (κ) remained unchanged containing increasing silver nitrate content, which resulted in an obvious enhancement in the figure of merit (ZT) of the composites. Consequently, the maximum ZT of the AgNPs/PANI hybrid nanocomposites amazingly reached 5.73×10^{-5}, which is about 3.8 times of ZT of the pure PANI (1.503×10^{-5}). This study suggests that organic/low-dimensional metal particles hybridization is promising to effectively improve thermoelectric properties of conducting polymers.

Introduction

It is clear that the fossil energy comes to the edge of exhaustion, searching and developing new, clean, effective and reproducible energy turn to be an urgent issue. Thermoelectric (TE) materials can transfer energy between heat and electricity without mechanical device, making them reliable and simple, and are now attracting more and more attention from the worldwide scientific research community.[1] Furthermore, numerous advantages make it extensively apply in fields, such as waste heat recovery from the automobile hot exhaust stream, thermoelectric refrigeration and so on.[2] The performance of thermoelectric material is determined by its dimensionless figure of merit ZT. A good thermoelectric material should possess high σ, large S and low κ, where high Seebeck coefficient provides high voltage in thermal power generators, large electrical conductivity minimizes Joule heating and low thermal conductivity reduces heat losses.[3-5] In addition, the power factor ($S^2\sigma$), which determines the electrical performance of thermoelectric materials, can also reflect the pros and cons of thermoelectric properties.

Currently, a lot of TE materials including inorganic semiconductors, such as PbTe, Bi_2Te_3, $CoSb_3$ and their alloys, have been applied practically. However, most inorganic thermoelectric materials are prepared by melt growth (arc melting method, zone melting, melt-annealing) and powder metallurgy method that involves high temperature, long-term and high-cost fabrication processes. Compared with inorganic thermoelectric materials, organic thermoelectric materials, which has been widely considered as a potential candidate for TE materials, have intrinsically low thermal conductivity, low toxicity, mechanical flexibility and inexpensive processability. [6-10,59]

Usually, organic conducting polymers such as polyaniline (PANI), poly (3,4-ethylenedioxythiophene), poly (styrenesulfonate) (PEDOT:PSS), polythiophene (PTH), polycarbazoles (PC), polypyrrole (PPY) and polyacetylene (PA) are aviliable to TE devices.[11-20] Particularly, due to the low cost, structural diversification, unique doping/dedoping progress, low thermal conductivity, and the nature of easy to synthesis, PANI is regarded as one of the most potential effective and suitable TE material among conducting polymers. Low electrical conductivity and Seebeck coefficient, however, lead to the serious lag of its large-scale application. Practice application has employed different methods to improve the TE properties of PANI，among which one approach is to prepare organic/ inorganic hybrid material so as to adjust the carrier concentration, achieving high ZT performance. In the last decade, metal oxides, metals and carbon materials have been introduced into PANI matrix to enhance its thermoelectric properties.[20-22] Wu et al. have prepared $(PANI)_XV_2O_5{\bullet}nH_2O$, whose room-temperature conductivity was in the range of 10^{-4} to 10^{-1}S/cm and found that its thermoelectric power factor was from -30 to -200μV/k.[23] Anno et al. have fabricated polyaniline (PANI)/Bi-nanoparticles composites by a planetary ball-milling technique.[24] Yao et al have prepared

single-walled nanotubes/PANI nanocomposites through in situ polymerization.[25] Segregated-network carbon nanotube (CNT)-polymer composites were prepared by Yu et al.[26] Polyaniline/$NaFe_4P_{12}$ whisker and polyaniline/$NaFe_4P_{12}$ nanowire composites were prepared by a in situ compounding method.[27] Chatterjee et al. have synthetised structure-ordered cable-like polyaniline-bismuth telluride nanocomposites, which ZT value came to 0.0043.[28] A Ag_2Te/PANI core–shell thermoelectric nanostructure was reported by Wang et al.[29] Chen et al. have reported thermoelectric performance of ATT/TiO_2/PANI nanocomposites doped with different acids.[30] Graphite oxide (GO)/ordered-polyaniline (PANI) composites have been prepared through in situ polymerization, whose maximum thermoelectric figure of merit is up to 4.86×10^{-4}, 2 orders of magnitude higher than that of pure PANI.[31] Recently, we reported the synthesis of multi-walled carbon nanotube/polyaniline (MWCNT/PANI) hybrid nanocomposites by cryogenic grinding (CG) and spark plasma sintering (SPS).[32] It has been proved that the electrical properties of MWCNT/PANI composites are far better than those of pure PANI. Although their electrical conductivity reaches up to 1.59×10^2S/m, MWCNT content increases to 30wt%. The reason is that CNTs exhibit a rich variety of attractive electronic properties, such as metallic and semiconducting behaviour.

Metal silver is considered to have the best electrical and thermal conductivity among metals.[33] Due to this important characteristic，nano-sized silver has become the focus of scientific community of TE materials, making it favourite in practical application as conductive inks, thick film pastes, catalysis, sensing devices and dielectric material.[34-39] And the fabrication of Ag/PANI composites is very active recently because the incorporation of Ag into PANI can result in new composite materials with enhanced electronic properties. For example, Stejskal. J. have proposed four basic strategies for the preparation of the composites of conducting polymers and silver.[40] Du J. et al. have prepared Ag/polyaniline core-shell particles.[41] Silver–Polyaniline nanocomposites also have been fabricated through Gamma Radiolysis Method.[42] The oxidation of aniline with silver nitrate to polyaniline–silver composites was studied by Blinova N. V. et al.[43-44]

In this study, we prepared AgNPs/PANI hybrid nanocomposites via a one-pot method using $AgNO_3$ as a precursor, DBSA as a dopant, and APS as an oxidizing agent. It is the first time that this composite was treated as thermoelectric material. AgNPs were directly reduced without any assistance reducing agent. The as-prepared composite powder was consolidated by spark plasma sintering (SPS). Field-emission scanning electron microscopy (FESEM) and transmittance electron microscopy (TEM) images show that AgNPs with average size of 20-150nm are well distributed in the PANI matrix. The thermoelectric properties of the as-prepared AgNPs/PANI hybrid nanocomposites samples were investigated and the maximum ZT of the AgNPs/PANI hybrid nanocomposites was found to be 3.8 times higher than that of pure PANI.

Experimental Section

Materials Synthesis

Aniline (99.9%, monomer), Silver nitrate ($AgNO_3$, 99.9% Aldrich grade) and ammonium peroxydisulfate (APS, initiator) comesfrom Sinopharm Chemical Reagent Co., Ltd and DBSA (AR grade) Kanto. Particularly, the aniline cann't come into use until it is distill-purified. Corresponding solutions were prepared using deionized water during the synthesis process.

Solution A：Add 11g DBSA into distilled water (600ml) in round bottom flask under constant vigorous stirring for one hour to get aqueous micellar. Solution B: Dissolve 3g pro-cooled solution of aniline monomer in 50ml deionized water. After the solution A and B was mixed together, the mixture was stirred for half an hour. silver nitrate (0, 0.001M, 0.002M, 0.003M, 0.004M) were separately dissolved in 50ml of deionized water. And add them into above different solution. Dissolve silver nitrate (0, 0.001M, 0.002M, 0.003M, 0.004M) in 50ml of deionized water, then put them into the mixed solution mentioned above. 7.5g ammonium peroxydisulfate (APS) was dissolved in a 250ml beaker with 100ml deionized water as solution C. And transfer C into round bottom flask and freeze them at 0℃ for 8h. The resulting product was demulsificated of emulsion with large amount of methyl alcohol and then filtered with deionized water washing several times, finally make it freeze-drying at -80℃ refrigerant air drier for 48h. The as-prepared composite powder was consolidated at room temperature for a dwell time of 10 min by Spark Plasma Sintering (SPS, Dr.Sinter 725, Sumitomo Coal Mining Co., Tokyo, Japan).

Characterization

The phase purity of all AgNPs/PANI hybrid nanocomposites was examined by X-ray powder diffraction (XRD, Rigaku D/Max-2550PC, Japan) using Cu Kα radiation at 40kV, 200mA. The structure of polyaniline and AgNPs/PANI hybrid nanocomposites samples was characterized by a Nicolet 8700 FTIR spectrometer (FTIR, Thermo Fisher/Nicolet 6700, USA). The spectra was collected by the averaging of 32 scans ranging from 500 to 4000cm^{-1}. Then finely samples were placed into the ultraviolet and visible spectrophotometer (UV-Vis, PerkinElmer/Lanbda A35, USA) at room temperature to get absorption spectra. Field-emission scanning electron microscopy (FESEM, HITACHI/S-4800, Japan) and transmission electron microscopy (TEM, JEOL/JEM-2100F, Japan) were employed to investigate the morphology and microstructure of the sample.

The thermoelectric properties of as-prepared bulk samples were measured at 300-380K. And the electric resistance and Seebeck coefficient were investigated by a Seebeck Coefficient/Electric Conductivity Measuring System (ZEM-3, ULVAC-RIKO, Japan). The thermal diffusivity was investigated by a laser-flash method on a disk using a commercial system (Netzsch Instruments/LAF-457, Germany). The density of the composites was measured by the Archimedes method (METTLER TOLEDO/AL104, Switzerland). Measurement of the heat capacities (C_p) was accomplished through Differential Scanning Calorimetry (DSC, Netzsch/STA409PC, Germany). The values of the thermal conductivity are calculated according to:

$$\kappa=\lambda\rho C_p \quad (1)$$

where λ is the thermal diffusivity, ρ is the density and C_p is the heat capacity.

Results Discussion

Morphology Characterizations

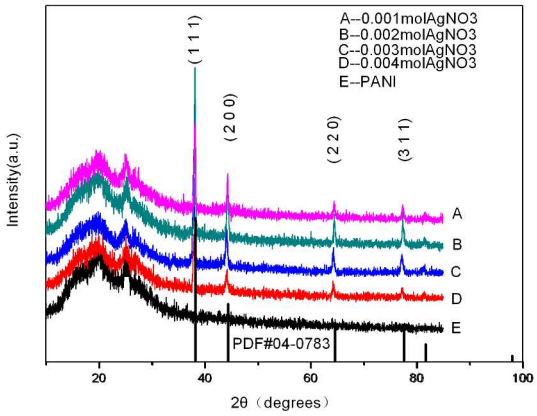

Fig.1. X-ray diffractograms of AgNPs/PANI hybrid nanocomposites with different contents silver nitrate

Fig.1 shows the X-ray diffraction patterns of AgNPs/PANI hybrid nanocomposites with different silver nitrate contents. The broad peak at 2θ=19.578°, 25.402°, which suggests the existence of the PANI can be attributed to the periodicity parallel to the amorphous polymer chain.[45] The sharp peaks at 2θ values 38.179°, 44.340°, 64.50°, 77.40°, 81.561°, corresponding to (1 1 1), (2 0 0), (3 1 1) and (2 2 2) respectively, can be regarded as the pure phase of Ag (JCPDS File No. 04-0783).[46] In sum, the information mentioned above clearly indicates the AgNPs exist in the composites with their crystalline nature.

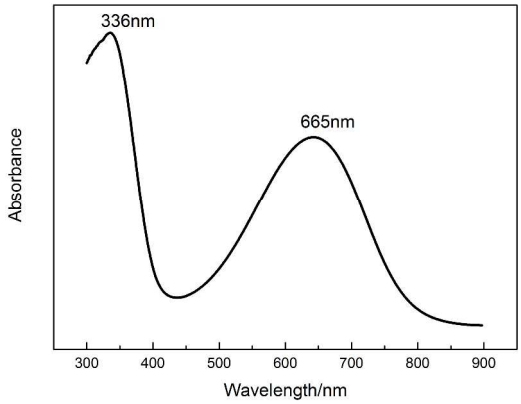

Fig.2. UV-vis spectra of AgNPs/PANI hybrid nanocomposites with 0.004M silver nitrate

For the reduction of $AgNO_3$, the amine nitrogen is selected to act as sites for reducing the Ag^+. The sonication-drived AgNPs/PANI hybrid nanocomposites in N-methylpyrrolidone were studied by UV-vis spectroscopy, as shown in Fig.2. The peak at ~336nm corresponds to surface plasmon resonance (SPR) of the AgNPs embedded in the polymer matrix.[39,47,48] The maximum absorption peak was at approximately 665nm, corresponding to the π-π* transition of quinoneimine rings.[43]

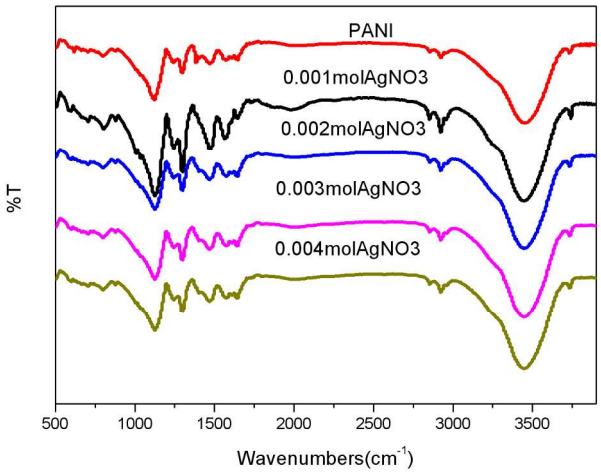

Fig.3. FTIR of AgNPs/PANI hybrid nanocomposites with different contents silver

Fig.3 shows the FTIR spectra of AgNPs/PANI hybrid nanocomposites with different silver nitrate contents. The characteristic band centred at 665 cm^{-1} corresponds to the C–S stretching of the benzenoid ring of DBSA.[45] The peaks at 1297cm^{-1} and 1241cm^{-1} are assigned to C-N stretching of the second amine of PANI backbone and the characteristic of the conducting PANI emeraldine salt (ES) form, respectively. The band at 1130cm^{-1} indicates an in-plane bending vibration of C-H (mode of N=quinoid=N, quinoid=N+H-B, and B-N+H-B), which is formed during protonation. We assign the peak ranging from 2700 to 3000cm^{-1} to aliphatic C-H stretching mode, depending on long alkyl tail of DBSA.[49] The bands near 1485 and 1570 cm^{-1} respectively correspond to C=C stretching of the benzenoid and quinoid rings.[50] We observe that there is a shift in the peaks associated with C=N and C=C stretching of quinoid ring compared to pure PANI, which is as reported in the literature[35], and no appreciable change in peak position is detected for benzenoid ring. Therefore, we conclude that Ag^+ reside close in the imine nitrogen of the PANI and be reduced to AgNPs.[48]

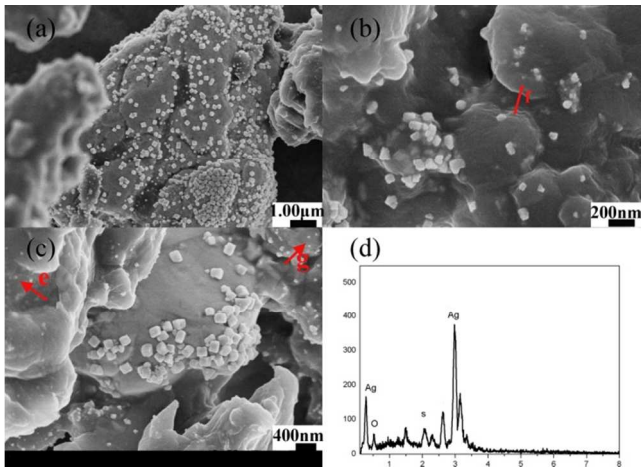

Fig.4. FESEM image (a-c) and elemental analysis (d) of AgNPs/PANI hybrid nanocomposites with 0.004M silver nitrate

Table 1 Elemental composite of AgNPs/PANI hybrid nanocomposites with 0.004M silver nitrate

El	AN	Series	unn. [wt.%]	C Atom. [at.%]
Ag	47	L-series	85.41	51.06
C	6	K-series	4.28	22.95
O	8	K-series	5.16	20.78
S	16	K-series	2.59	5.20

Typical low and high magnification FESEM micrographs of AgNPs/PANI hybrid nanocomposites with 0.004M silver nitrate can be observed in Fig.4. The images show that the AgNPs are well dispersed in PANI matrix and the diameter of AgNPs is about 40-150nm. Meanwhile, some small AgNPs can also be recognized as identified with red arrow in Fig 4 (e,f,g). The EDS spectra (Fig.4d) and elemental composition (Table 1) show the presence of Ag, O and S, which respectively indicates the presence of AgNPs in the nanocomposites and that O and S exist in PANI matrix.

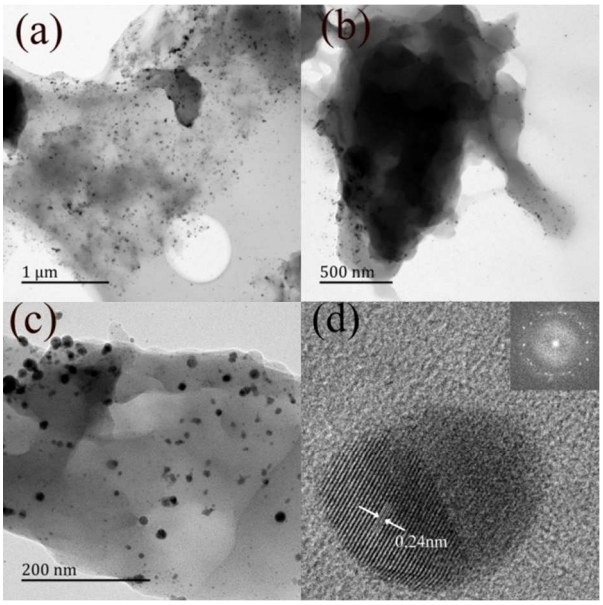

Fig.5. TEM image (a-c) and elemental analysis (d) of AgNPs/PANI hybrid nanocomposites with 0.004M silver nitrate.

Fig.5 shows a typical TEM image (Fig.5a-c) of AgNPs/PANI hybrid nanocomposites with 0.004M silver nitrate and the AgNPs, whose particle size is approximately 20-30nm, are well dispersed in PANI matrix. It is clear that these small AgNPs well match with those observed by FESEM (pointed with red arrow). In fact, the size distribution of AgNPs is broad and about 20-160nm in this work, as shown in Fig 4 and Fig 5. Due to the impact of labile factors in the synthesis process, the results showed a big difference in the size of the AgNPs. In this process, the silver ions were absorbed onto the imine nitrogen of the PANI and then reduced to AgNPs. We did not use surfactants to prevent AgNPs from unrestricted growth, which results in a different size distribution of AgNPs. SEM images show that the diameter of AgNPs is about 60-150nm, but some much smaller AgNPs could be found in PANI matrix from Fig 4, thus the size of AgNPs in Fig 5c and Fig 5d is about 20-30 nm. The clear and uniform lattice fingers spacings (Fig.5d) 0.24nm agree with the interplanar distance the (1 1 1) lattice planes of Ag.

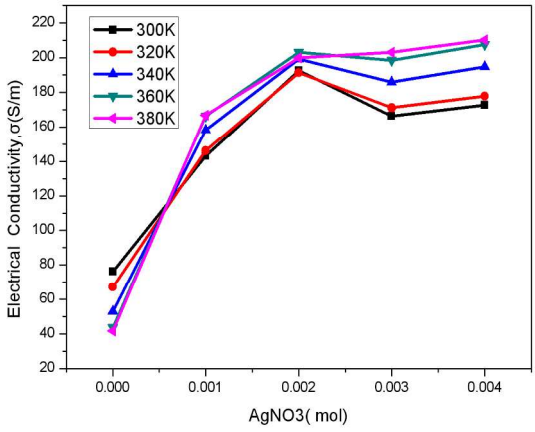

(a)

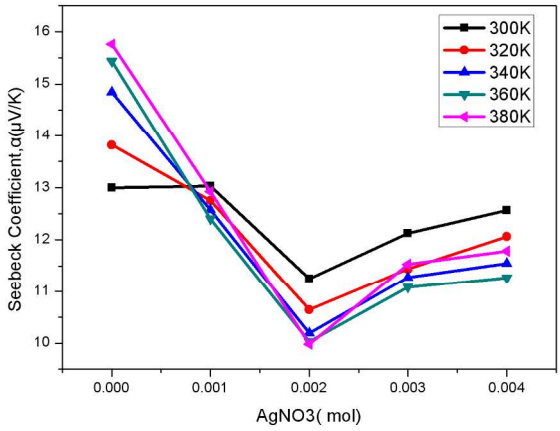

(b)

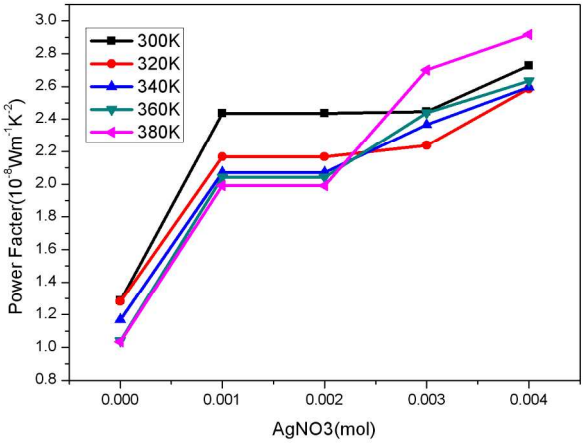

(c)

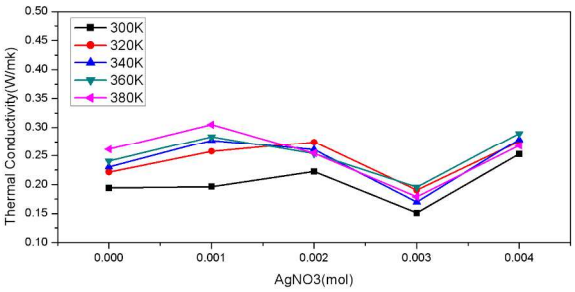

(d)

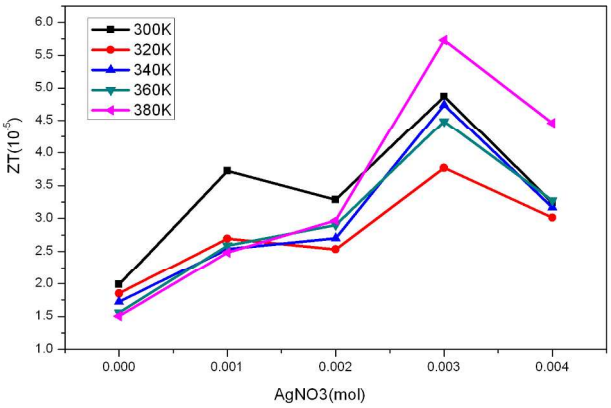

(e)

Fig.6. The electrical conductivity (a), the Seebeck coefficient (b), the power factors (c), (d) the thermal conductivity values and the ZT value(e) of AgNPs/PANI hybrid nanocomposites with different contents silver

Thermoelectric properties

The thermoelectric properties of the AgNPs/PANI hybrid nanocomposites were measured in the temperature ranging from 300K to 380K, as displayed in Fig6. It can be observed that the electrical conductivity of the AgNPs/PANI hybrid nanocomposites also increases dramatically with increasing silver nitrate content and finally reaches 2.10×10^{2}S/m with the silver nitrate content of 0.004M at 380K, which is more than 2.75 times larger than that of pure PANI. The enhancement of the electrical conductivity ($\sigma=ne\mu$, where n is the carrier concentration, e is the electron charge and μ is the carrier mobility) can be attributed to the introduction of AgNPs in the PANI matrix, to provide the silver islands lowering the carrier hopping barriers and increasing the charge transfer channel and carrier concentration of the nanocomposites. While the Seebeck coefficient decreases with the increasing contents of silver nitrate. Since the Seebeck

$$S = \frac{S_1\sigma_1 + S_2\sigma_2}{\sigma_1 + \sigma_2} \quad (2)$$

For a composite with high impurity content, the effective thermopower would be dramatically decreased because the small-thermopower term on the right of Eq. (2).[58] The power factor ($S^2\sigma$) of the nanocomposites changed from 1.03×10^{-8}Wm^{-1}K^{-2} to 2.91×10^{-8} Wm^{-1}K^{-2} at 380K with increasing silver nitrate contents. Fig.5(d) shows that there is no obvious change in the thermal conductivity value, which remains in low values in the range of 0.150-0.305W/mK. The total thermal conductivity can be calculated by $\kappa_{total}=\kappa_e+\kappa_l$, where κ_e is the electronic contribution and κ_l is the lattice contribution.The latter κ_l can be reduced by selective scattering of phonons through the form of nanoscale inclusions in nanostructure.[28,51-54] In the AgNPs/PANI hybrid nanocomposites, the PANI and Ag nanoparticles nanostructure provides many nano-interfaces to scatter phonons selectively, decreasing κ compared with bulk silver (the thermal conductivity of metal silver is 430W/mK[54]) and not increasing greatly compared with pure PANI. The highest ZT value is 5.73×10^{-5} at 380K for AgNPs/PANI hybrid nanocompasites with 0.003M silver nitrate. Although the ZT of the AgNPs/PANI is not competitive with other PANI-based composites, Ag wt% is just 6.4% in our composites. In other PANI-based composites, for example in MWCNTs/PANI, the MWCNTs wt% is more than 30%.[32] In GO/PANI, the GO wt% is more than 40%.[31] In SWNT/PANI, the SWNT wt% is more than 40%.[25] Meanwhile, we can speculate the ZT changing trends of the AgNPs/PANI would increases with increasing silver nitrate content from Fig.6.(a)(c)(e).

Fabrication and conductive mechanism

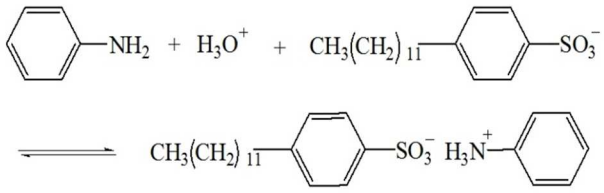

(a)

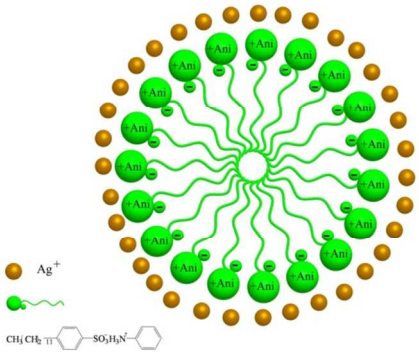

(b)

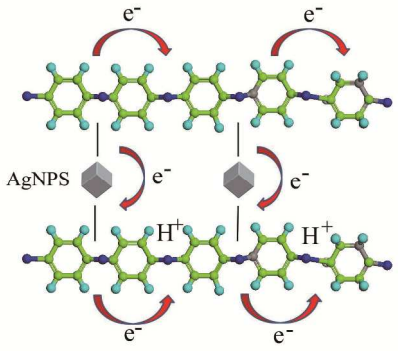

(c)

Fig.7 (a)(b)(c). Schematic representation of AgNPs/PANI hybrid nanocomposites

The increase of electrical conductivity in the AgNPs/PANI hybrid nanocomposites is attributed to the incorporation of AgNPs. A possible mechanism of the conductivity enhancement can be explained through the information in Fig.7. Firstly, the aniline monomer reacts with DBSA then the resulting product forms anilinium cation with a long alkyl tail as shown in the Fig.7(a). As the reaction time prolongs, anilinium cations diffuses into DBSA to be anilinium cation-DBSA micelle. And then homodispersed silver ions were attached to the imine nitrogen of the micelle by absorbtion. Then the reaction product anilinium cation-DBSA micelle serves as the template for silver ions, as shown in the Fig.7(b). After that, the silver ions were directly reduced to AgNPs. Meanwhile aniline was oxidated with $AgNO_3$ in DBSA, but this process was slow and it took months.[43] After APS was added into the solution, anilinium cation-DBSA micelles were rapidly transformed into PANI through a series of chain reactions. In the detection results, it is clear that these in-situ synthesized AgNPs were distributed uniformly in PANI matrix, which could be confirmed by FESEM (Fig.4) and TEM image (Fig.5). Silver has excellent electrical conductivity, so we deduced that AgNPs increased the carrier transport path as a conducting bridge not only in the intramolecular but also intermolecular chains, as shown in the Fig.7(c). Usually, the carrier transport in pure PANI is principally controlled by the interchain and intrachain hopping processes and the transport behavior follows the variable range hopping (VRH) model.[52] Adding AgNPs into the PANI matrix formed new conductive channel, enhanced the carrier mobility, shorted carrier hopping distance and especially improved the carriers interchain transfer efficiency, thus AgNPs can effectively improve the conductivity of the AgNPs/PANI hybrid nanocomposites. The conduction mechanism is similar to the one reported in ref. et.al.[48,57]

Conclusions

This study has described the fabrication and characterization of AgNPs/PANI hybrid nanocomposites in details prepared via a one-pot method. The XRD, FESEM and TEM results show AgNPs was synthesized successfully and embedded uniformly in the PANI matrix. As the silver nitrate content increased from 0.001M to 0.004M, the electrical conductivity of AgNPs/PANI hybrid nanocomposites increased from 0.416×10^{2}S/m to 2.10×10^{2}S/m, the thermal conductivity still kept low values about 0.25 W/mK and the maximum ZT reached 5.73×10^{-5}. Meanwhile we proposed a speculation of the mechanism of AgNPs/PANI hybrid nanocompasites. These materials has experimentally demonstrated that the existence of AgNPs truly improve thermoelectric properties of PANI.

Acknowledgements

This work was funded by Natural Science Foundation of China (No. 51374078), Shanghai Committee of Science and Technology (No. 13JC1400100), "Shu Guang" project supported by Shanghai Municipal Education Commission and Shanghai Education Development Foundation (No.11SG34), Shanghai Rising-Star Program (No.12QH1400100) , PCSIRT (No.IRT1221), the Fundamental Research Funds for the Central Universities, and DHU Distinguished Young Professor Program in University.

Notes and references

State Key Laboratory for Modification of Chemical Fibers and Polymer Materials, Donghua University, 2999 North Renming Road, Shanghai 201620, PR China.; E-mail: wanglj@dhu.edu.cn

1 H.K. Lyeo, A. Khajetoorians, L. Shi, K.P. Pipe, R.J. Ram, A. Shakouri, C. Shih, *Science*, **2004**, *303*, 816.
2 A. Minnich, M. Dresselhaus, Z. Ren, G. Chen, *Energy Environ Sci*. ,**2009**, *2*, 479.
3 G.S. Nolas, J. Sharp, H. Goldsmid, "Thermoelectrics: Basic Principles and New Materials Developments", Springer, New York, **2001**.
4 C. Bounioux, P. Chao, M. Quiles, M.S. González, A.R. Goñi, R. Rozen, C. Müller, *Energy Environ Sci*., **2013**, *6*, 918.
5 D.M. Rowe, "Thermoelectrics handbook: macro to nano", CRC press, **2006**.
6 J.P. Heremans, V. Jovovic, E.S. Toberer, A. Saramat, K. Kurosaki, A. Charoenphakdee, S. Yamanaka, G.J. Snyder, *Science*, **2008**, *321*, 554.
7 Y. Min, J.W. Roh, H. Yang, M. Park, S.I. Kim, S. Hwang, S.M. Lee, K.H. Lee, U. Jeong, *Adv. Mater*., **2013**, *25*, 1425.
8 D.V. Talapin, C.B. Murray, *Science*, **2005**,*310*, 86.
9 J. Yang, B. Xu, L. Zhang, Y. Liu, D. Yu, Z. Liu, J. He, Y. Tian, *Mater. Lett*., **2013**, *98*, 171.
10 G.H. Kim, L. Shao, K. Zhang, K.P. Pipe, Nat. Mater., 2013,12,719.
11 Y. Lu, Y. Song, F. Wang, *Mater. Chem. Phys*., **2013**, *138*, 238.
12 H. Anno, M. Hokazono, F. Akagi, M. Hojo, N. Toshima, *J. Electro. Mater*., **2013**, *43*, 1346.
13 M.O. Ansari, M.M. Khan, S.A. Ansari, I. Amal, J. Lee, M.H. Cho, *Mater. Lett*., **2014**, *114*, 159.
14 H. Song, C. Liu, H. Zhu, F. Kong, B. Lu, J. Xu, J, Wang, F. Zhao, *J. Electro.Mater*., **2013**, *42*, 1268.
15 Q. Jiang, C. Liu, H. Song, H. Shi, Y. Yao, J. Xu, G. Zhang, B. Lu, *J. Mater. Sci-Mater. El.*, **2013**, *24*, 4240.
16 H. Song, F. Kong, C. Liu, J. Xu, Q. Jiang, H. Shi, *J. Polym. Res.*, **2013**,*20*,1.
17 Y. Hu, H. Shi, H. Song, C. Liu, J. Xu, L. Zhang, Q. Jiang, *Synthetic Met.*, **2013**, *181*, 23.
18 L. Wang, X. Jia, D. Wang, G. Zhu, J. Li, *Synthetic Met.*, **2013**, *181*, 79.
19 G.Zotti, G.Schiavon, S. Zecchin, J.F. Morin, M. Leclerc, *Macromolecules*, **2002**,*35*, 2122.
20 Y. Du, S.Z. Shen, K. Cai, P.S. Casey, *Prog. Polym. Sci*., **2012**,*37*, 820.
21 L. Yan, M. Shao, H. Wang, D. Dudis, A. Urbas, B. Hu, *Adv. Mater.*, **2011**, *23*, 4120.
22 G. Ćirić-Marjanović, *Synthetic Met*., **2013**,*170*, 31.
23 C.G. Wu, D. DeGroot, H. Marcy, J. Schindler, C. Kannewurf, Y.J. Liu, W. Hirpo, M. Kanatzidis, *Chem. Mater*., **1996**,*8*,1992.
24 H. Anno, M. Fukamoto, Y. Heta, K. Koga, H. Itahara, R. Asahi, R. Satomura, M. Sannomiya, N. Toshima, *J. Electro.Mater*., **2009**, *38*, 1443.
25 Q. Yao, L. Chen, W. Zhang, S. Liufu, X. Chen, *ACS Nano*, **2010**, *4*, 2445.
26 C. Yu, Y.S. Kim, D. Kim, J.C. Grunlan, *Nano Letters*, **2008**, *8*, 4428.
27 H. Liu, J. Wang, X. Hu, R.I. Boughton, S. Zhao, Q. Li, M. Jiang, *Chem. Phys. Lett*., **2002**, *352*, 185.
28 K. Chatterjee, M. Mitra, K. Kargupta, S. Ganguly, D. Banerjee, *Nanotechnology*, **2013**, *24*, 215.
29 Y. Wang, K. Cai, J. Yin, Y. Du, X. Yao, *Mater. Chem. Phys.*, **2012**,*133*, 808.
30 L. Chen, Y. Zhai, H. Ding, G. Zhou, Y. Zhu, D. Hui, *Compos. Part. B-Eng.*, **2013**,*45*, 111.
31 Y. Zhao, G.S. Tang, Z.Z. Yu, J.S. Qi, *Carbon*, **2012**,*50*, 3064.
32 Q. Zhang, W. Wang, J. Li, J. Zhu, L. Wang, M. Zhu, W. Jiang, J. *Mater. Chem. A*., **2013**,*1*, 12109.

33 Y. Sun, Y. Xia, *Nature*, **1991**. *353*, 737.
34 J. Kim, J. Cho, S. Chung, J. Kwak, C. Lee, Y. Hong, J. J. Kim, J. Korean. *Phys. Soc*., **2009**,*54*, 518.
35 H. Lu, H. Xu, Y. Chen, J. Zhang, J. Zhuang, *Rsc Advances,* **2014**, *4*, (12), 5873-5879.
36 A. Choudhury, *Sensor Actuat B: Chem.*, **2009**,*138*, 318.
37 K.Cao, X.M.Jiang, S.T.Yan, L.Y.Zhang, W.T.Wu, *Bios. Bioelectron.*, **2014**, *54*, 188.
38 F. Yakuphanoglu, E. Basaran, B. Senkal, E. Sezer, *J. Phys. Chem. B*, **2006**, *110*, 16908.
39 M.S. Tamboli, M.V. Kulkarni, R.H. Patil, W.N. Gade, S. C. Navale, B.B. Kale, *Colloid. Surface. B*, **2012**, *92*, 35.
40 J. Stejskal. *Chemical Papers*, **2013**, *67*, (8), 814-848.
41 M. N. Nadagouda, R. S. Varma. *Macromolecular Rapid Communications*, **2007**, *28*,(21), 2106-2111.
42 K. Mallick, M. J. Witcomb, A. Dinsmore, M.S. Scurrell, *Macromolecular rapid communications*, **2005**, *26*, (4), 232-235.
43 N.V. Blinova, J. Stejskal, M. Trchová, I. Sapurina, G. Ciric-Marjanovic， *Polymer*， **2009**, *50*, (1), 50-56
44 N.V. Blinova，P. Bober, J. Hromádková, M. Trchová, J. Stejskal, J. Prokeš, *Polymer International*, **2010**, *59*, (4), 437-446.
45 M.R. Karim, C.J. Lee, Y.T. Park, M.S. Lee, *Synthetic Met*, **2005**,*151*, 131.
46 C. Chen, L. Wang, G. Jiang, J. Zhou, X. Chen, H. Yu, Q. Yang, *Nanotechnology*, **2006**,*17*, 3933.
47 L.M. Huang, C.C. Tsai, T.C. Wen, A. Gopalan, *J. Poly. Sci. Pol. Chem.*, **2006**, *44* 3843.
48 B. Bhowmick, D. Mondal, D. Maity, M.M.R. Mollick, M.K. Bain, N.K. Bera, D. Rana, S. Chattopadhyay, D. Chattopadhyay, *J. Appl. Polym. Sci.*, **2013**,*129* ,3551.
49 A. Milton, A. Monkman, *J. Physics D Appl. Phy.,* **1993**, *26*, 1468.
50 M.G. Han, S.K. Cho, S.G. Oh, S.S. Im, *Synthetic Met.,* **2002**,*126*, 53.
51 A.B. Afzal, M. Akhtar, M. Nadeem, M. Ahmad, M. Hassan, T. Yasin, M. Mehmood, *J. Physics D Appl. Phy.*, **2009**,*42*, 015411.
52 M.S. Dresselhaus, G. Chen, M.Y. Tang, R. Yang, H. Lee, D. Wang, Z. Ren, J.P. Fleurial, P. Gogna, *Adv. Mater.*, **2007**,*19,* 1043.
53 J.R. Sootsman, H. Kong, C. Uher, J.J. D'Angelo, C.I. Wu, T.P. Hogan, T. Caillat, M.G. Kanatzidis, *Ange. Chemie,* **2008**, *120*, 8746.
54 A. Minnich, M. Dresselhaus, Z. Ren, G. Chen, *Energ. Environ. Sci.,* **2009**, *2*, 466.
55 R. Berman, F.E. Simon, J. Wilks, *Nature Lond,* **1951**, *168*, 277.
56 Y. Long, Z. Chen, X. Zhang, J. Zhang, Z. Liu, *Appl. Phy. Lett.,* **2004**, *85*, 1796.
57 R.J. Tseng, J. Huang, J. Ouyang, R.B. Kaner, Y. Yang, *Nano Letters,* **2005**, *5*, 1077.
58 X. Shi, L. Chen, S. Bai, X. Huang, X. Zhao, Q. Yao, C.Uher. *Journal of Applied Physics* **2007**, *102*, (10), 103709.
59 Q. Zhang, X. Ai, W. Wang, J. L. Wang, W. Jiang, *Acta Materialia.*, **2014**,*73*, 37-47.